Al-Meshragi, M. & Hughes, R., Journal of the Association of Arab Universities for Basic and Applied Sciences, Vol.3, 2007, 33-47

An Investigation of the Wall Heat Transfer in Fixed Bed Reactor at Atmospheric and High Pressure

Al-Meshragi[a], M. & Hughes[b], R.

[a] *Chemical Engineering Department; Faculty of Engineering; Al-Mergheb University, Alkhoms-Libya; P.O. Box 303, Zliten / Libya*
moh_almeshragi@yahoo.com
[b] *Chemical Engineering Department; Salford University, Manchester-UK.*

ABSTRACT

A wall heat transfer parameters in fixed bed in a radial direction using air, carbon dioxide and helium has been measured. In addition, the radial wall heat coefficient in the same fixed bed was investigated under high pressure (up to 20 bar). The temperature gradients obtained from the experimental data were analyzed by the two-dimensional pseudo-homogeneous model to determine the wall heat transfer coefficient. The results obtained from experimental data for atmospheric and high pressure indicates that the wall heat transfer coefficient increase with increasing Reynolds number at both pressures. However, the effect of pressure upon wall heat transfer coefficient as function of Reynolds number indicates that pressure higher than atmospheric cause a decrease in the wall heat transfer and the values of atmospheric pressure were found to lie well above those at high pressures.

KEYWORDS: Wall heat transfer coefficient; packed bed; pseudo-homogenous model; pressure effect.

INTRODUCTION

Knowledge of the radial heat transfer mechanism through the packing and the wall for fluid flowing through a single tube forms an important aspect of the design of fixed bed reactors. In fixed bed reactors, when exothermic reactions are processed, it is essential to remove sufficient heat to limit the reaction temperature and thus reduce the possibility of parasitic reactions and thermal degradation of the catalyst by sintering. On the other hand, endothermic reactions require sufficient heat to be supplied to prevent the reaction temperature from falling with a concomitant fall in conversion.

The mechanism of heat transfer inside the tube wall is via heat transferred through the solid particles adjacent to the wall by conduction, in addition to heat transferred by fluid convection. Moreover, the thermal properties of the bed and fluid have a significant effect on the condition and convection mode.

The rational design of fixed reactors is to ensure optimum conditions for these reactions by determining the temperature distribution within the reactor and the operational parameters such as the diameter of the reactor tube and the size of catalyst pellets.

Wall heat transfer can be estimated from steady state heat transfer experiments without reaction, which should provide approximate values under reaction conditions. Generally, however steady state heat transfer experiments without reaction known to be more reliable. In practice, under reaction conditions, these non-reactive estimates may have to be tuned in order to predict the observed radial and axial temperature profiles in the reactor.

EXPERIMENTAL WORK

In order to study the wall heat transfer coefficient in fixed–bed reactor the present apparatus was designed in such a way that allows the measurement of the temperature profiles above the beds at high and atmospheric pressures.

Design of the Reactor

The heat exchanger reactor tube was constructed from stainless steel which is suitable for pressures up to 103.42 bars. The reactor assembly comprised is shown in Figure (1). The lower section or calming section (50.8 mm i.d. & 360 mm in length) was surrounded by a jacket through which a tap water at room temperature is passed. Stainless steel rasching rings (5.56 mm diameter) were packed in order to obtain a uniform velocity and temperature profile to the test section. The two sections are separated from each other by a gasket of low thermal conductivity in order to minimize any heat escape to the lower section.

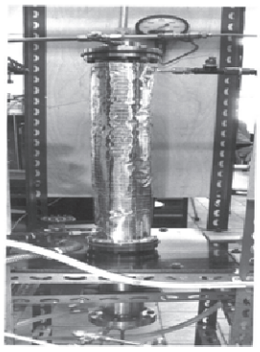

Figure 1. Fixed Bed Reactor

Thermocouple Cross and Fabrication

The radial temperature profile is measured using thermocouples mounted on a cross as illustrated in Figure 2. The cross itself is incorporated with stainless steel tubing, which can be moved vertically within the reactor. The top and bottom of the tube holder was covered and then welded with a piece of mesh.

The eight thermocouples (chromel-alumel of 0.5mm diameter) were placed at different distances from the center of the cross through the middle of a hypodermic tube. The thermocouples were arranged as r = 10, 15, 20, 25, 30, 35, 40 and 45mm, from the center of the cross stainless steel tube (3.16mm o.d. and 1.24mm i.d.), which was welded at the center of the cross to keep the tube holder firmly held and avoid any fluidization at high flow rates. The central thermocouple was then inserted through the cross. A ninth thermocouple was attached to the stainless steel tube holder at the wall to record the inside wall temperature reactor.

The nine thermocouples were led through the top of the reactor by a telescopic arrangement of tubes (a 9.5mm tube inside a 12.7mm tube). This enables the cross to be moved up or down. The hypodermic tube of (3.16mm o.d.) which contains the central thermocouple projects through the top telescopic arrangement. The thermocouples were then passed through the arm of the "T" fitting.

All fittings are of the compression type, with polypropylene olives used for sealing the hypodermic tube and the 9.5mm - 12.5mm telescope junction so as to allow the movement of

both the aforementioned pieces of equipment. The cross thermocouple leads, which used at high pressures, were sealed with silastomer rubber. This was found to be suitable for avoiding any gas leakage when the high pressure experiments were carried out.

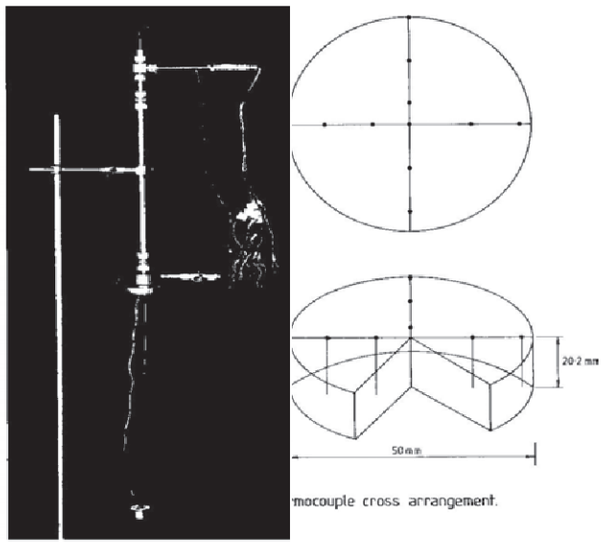

Figure 2. Thermocouple Probe

All thermocouples leads were connected to a μ-Data logger and then to the micro-computer. A computer program has been written to measure all these thermocouples.

CALCULATION OF WALL HEAT TRANSFER COEFFICIENTS

The two dimensional parameter continuum models, for conductive heat transfer, in a cylindrical packed bed operated as a steady state heat exchanger was used to evaluate the effective thermal conductivity and wall heat transfer coefficient. The over-all heat balance across the eliminated section of the cylindrical tube may be written as follows:

$$Heat_{input} = Heat_{output}$$

$$GC_pTA_2 + K_{cr}A_1\frac{\partial}{\partial z}(T+\frac{\partial T}{\partial r}) + K_{ea}A_2\frac{\partial}{\partial z}(T+\frac{\partial T}{\partial z}) \qquad (1)$$

$$= GC_pTA_2(T+\frac{\partial T}{\partial z}) + K_{er}A_3\frac{\partial T}{\partial r} + K_{ea}A_2\frac{\partial T}{\partial z}$$

After simplification and re-arrangement of Equation 1, the differential equation for steady state heat transfer in a non-adiabatic packed bed becomes:

$$K_{er}(\frac{\partial^2 T}{\partial r^2} + \frac{1}{r}\frac{\partial T}{\partial r}) + K_{ea}\frac{\partial^2 T}{\partial z^2} = GC_p\frac{\partial T}{\partial z} \qquad (2)$$

where,

K_{ea}= effective axial thermal conductivity.

Since the heat transferred axially by conduction is small compared to that carried by the mass flow of the gas, Equation 2 can be simplified even more by neglecting the ($\partial^2 T/\partial z^2$) term. Then Equation 2 will be taken as the following form:

$$K_{er}\left(\frac{\partial^2 T}{\partial r^2}+\frac{1}{r}\frac{\partial T}{\partial r}\right)=GC_p\frac{\partial T}{\partial z} \tag{3}$$

The fundamental Equation 3 used for the analysis was based on the following assumption:

i. The mass velocity of the fluid is uniform across the tube diameter.
ii. The temperature difference between solid and fluid is negligible.
iii. The effective thermal conductivity is uniform with the bed.

Equation 3 can be intern grated with the boundary condition given by the methods outlined by Marshall (1951). The final form of Equation 3 can be written as:

$$\frac{T_w-T}{T_w-T_0}=2\sum\frac{J_0\left[\left(\frac{a_n}{R_t}\right)\exp(-a_n^2 Y)\right]}{a_n\left[1+a_n/\beta^2\right]J_1(a_n)} \tag{4}$$

where;

$$\beta=h_w R_t/K_{er} \tag{5}$$

$$Y=K_{er}Z/GC_pR_t^2 \tag{6}$$

J_o= Bessel function of zero order and first kind.
J_1= Bessel function of first order and first kind.

And ∂n is a nth root of the Bessel function J_o and J_1.

$$\beta j_o(a_n)=a_n J_1(a_n) \tag{7}$$

The effective radial thermal conductivity and wall heat transfer coefficient can be computed by using optimization routines programs.

The routines minimize the sum of the squares of the residuals of the theoretical and experimental temperature and the values of K_{cr} and h_w were then obtained by iteration from initial guesses of the bed exit temperatures.

$$F=\sum_{i=1}^{N}\sum_{1}^{M}(T_{\exp}-T_{calc})^2 \tag{8}$$

where;
N is the number of bed heights;
M is the number of the exit temperatures.
The parameters K_{er} and h_w, can be obtained by either Equations 5, 6.

The theoretical radial temperatures are compared to the experimental temperature until the difference between two successive "F" minimum is smaller than 0.001, and sum of the squares of the residual "F" was then calculated.

EXPERIMENTAL PROCEDURE

Atmospheric Pressure

Preliminary tests in a glass tube of the same internal diameter as the reactor, established the appropriate weights of each catalyst to give required weight in the reactor. The desired bed depth was then checked by measuring the distance from the top of the backings to the top of the test section, with a dipstick at several positions. Then the bed depths were found by normal subtraction. In case of monoliths, the matrices each (50.8mm long) were inserted into the pore of the test section one by one up to the required height.

The thermocouple cross was then lowered into the bed until it rested just on or above the backing. The upper thermocouple cross flange was then screwed tightly into the top test section flange.

Steam and water were turned on, condensate in the steam outlet to be vented via a valve into a bucket. The condensate was then shut off and the steam trap condensed the out coming steam from the reactor jacket. The pressure inside the jacket was kept constant by means of a control valve set at 36 psig. The catalyst bed was then allowed to heat up to reach the steady state. This was easily checked by monitoring the thermocouples every ten minutes. The time taken to reach the steady state is approximately from 2 to 3 hours. Steady state was considered to be achieved when there was no significant change in the exit gas temperature for at least ten minutes. At this stage the desired volumetric flow rate measured by suitable rotameters to pass through the inlet calming section and then allowed until the steady state was attained. Under these flow conditions it took about 45 minutes to 1 hour for the required steady state. Upon reaching steady state conditions all temperature were printed out on the printer attached to the computer. The inlet temperature of the gas was taken as the average of the three-thermocouple readings in the entrance to the test section ($z=0$ plane). The flow rate was then changed or the bed depth repacked as appropriate and the procedure was repeated.

High Pressure

A schematic diagram of the apparatus for high pressure operation is shown in Figure 3. The catalyst is poured into the reactor until the required bed depth was obtained. The cross assembly was then suitably adjusted so that the stainless steel cross holder just touched the top of the catalyst and the flanges were screwed together tightly and carefully. The water and steam supplies were set up. The catalyst beds were then allowed to heat up until a steady state was attained. Before the air cylinder was connected, the "vent needle valve" in the dome was opened so that any residual pressure therein allowed venting to atmosphere. After that all the pipes, valves, connections were closed, and then the reactor was checked suitably for high pressure operation.

The valve "v_2" was closed while "v_1" is kept opened. Air supplied from the cylinder was adjusted to less than required pressure. Immediately the "loading needle valve" was opened and the dome was then changed by air pressure. The loading needle was then closed and the pressure was recorded by using the pressure gauge "c".

The valve "v_2" opened, and the gas at pressure was allowed to pass through the reactor. The pressure inside the reactor was fixed at the desired pressure (11 or 20 bars). The "loading needle valve" was very gently cracked and the dome charged via the "loading connection" until the desired blown - off pressure was reached. Then the "loading needle valve" was quickly closed and checked all valves in dome are closed. If the dome pressure was found to be high then the vent needle valve can be opened very gently so that the dome slowly bled until the observed blow-off pressure was reached, when the vent needle valve was closed.

The outlet connection was linked using 19.0 mm plastic tube with the flow meters "K" or "L" to the measured flow rates.

The spring-loaded safety valve "E" was adjusted at the required pressure. It was set to operate by relieving excess to increase rather slowly in order to provide adequate warning so that normal conditions were not exceeded.

The bed was then allowed to reach steady state. The temperatures of the representative thermocouples were monitored at regular intervals and showed no change. All the readings of the thermocouples were printed out. The bed-depth was then changed or the flow-rate adjusted and the procedure was repeated as required.

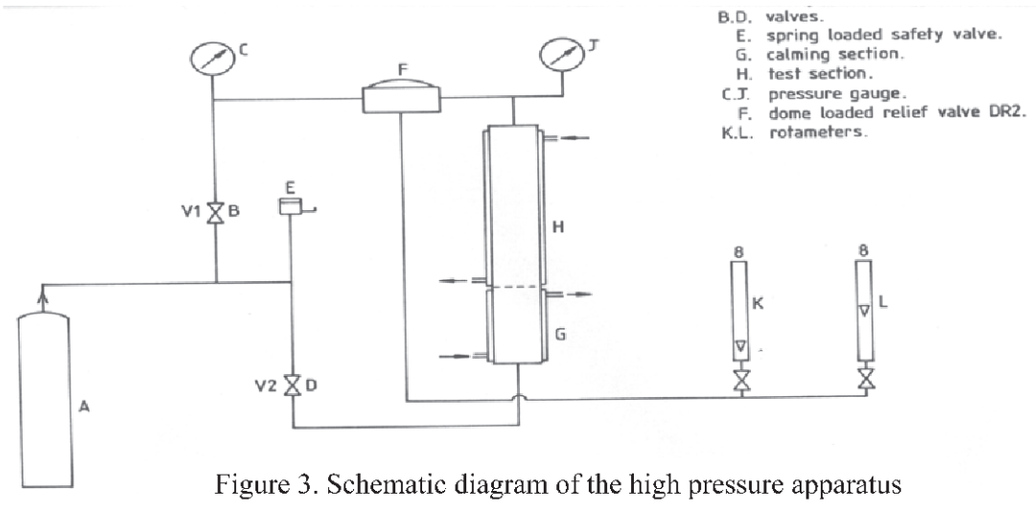

Figure 3. Schematic diagram of the high pressure apparatus

RESULTS AND DISCUSSION

The temperature profiles in the fixed bed reactor were found to be very sensitive to the wall heat transfer coefficient (h_w). The temperature profiles observed experimentally at different bed depths and 0.65 kg/m^2.s flow rate of air gas, were passed through beds comprising either catalyst pellets or monolith catalysts.

Radial temperature measurements are shown in Figures 4 to 9 which were plotted for 3 or 4 bed depths at constant flow rate for pelleted and monolith catalyst at atmospheric and elevated pressures. From the radial temperature profiles, shown in these Figures. the following features may be observed.

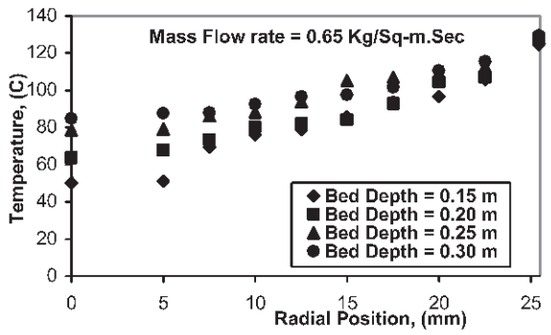

Figure 4. Radial temperature profiles at atmospheric pressure for (3.175*3.175) mm catalyst pellets using air

In some cases, the temperature profiles are far from smooth, suggesting that these could be dependent on the nature of the flow path within the reactor. It should be noted however, that the radial temperatures recorded refer to differential angular positions due to spiral positioning of the thermocouples in the cross. Thus these irregularities are to be expected.

For the pelleted beds and the monoliths a steep drop in the temperature, in the region from the wall to a point situated at a distance of about 2.5 to 5.0 mm from the wall, was observed in a number of the radial temperature profiles. This steep portion was clearly demonstrated especially at elevated pressures as shown in Figures 5 and 6 for pelleted catalyst and Figures 8 and 9 for the monolith catalyst.

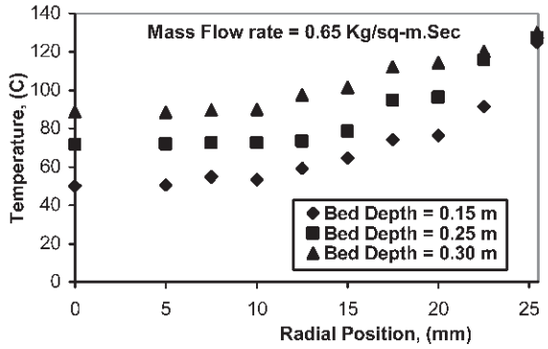

Figure 5. Radial temperature profiles at 11 bar pressure for (3.175*3.175) mm catalyst pellets using air

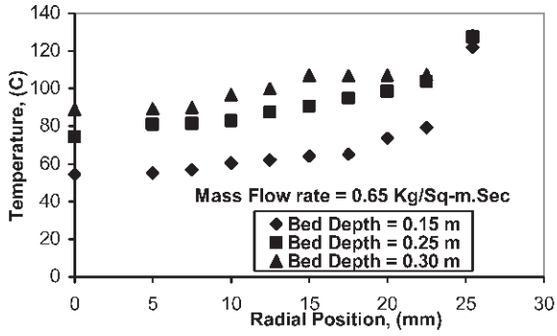

Figure 6. Radial temperature profiles at 20 bar pressure for (3.175*3.175) mm catalyst pellets using air

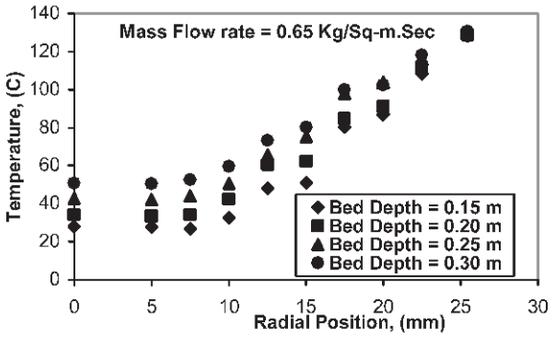

Figure 7. Radial temperature profiles at atmospheric pressure for monolith catalyst using air

The magnitude of the temperature drop near the wall increased sharply as the pressure within the reactor increased. The magnitude of this effect for ferroalloy monolith was very steep near the wall with the profiles in the bulk of the bed becoming flat as shown in Figure 8 and Figure 9.

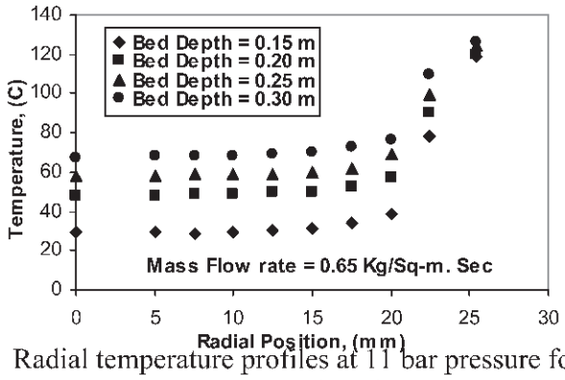

Figure 8. Radial temperature profiles at 11 bar pressure for monolith catalyst using air

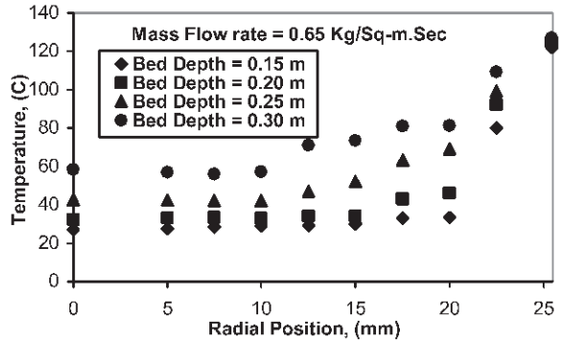

Figure 9. Radial temperature profiles at 20 bar pressure for monolith catalyst using air

A comparison between this steep drop near the wall for catalyst pellets beds and monoliths at elevated pressures shows that the magnitude of the temperature drop in the monolith catalyst was steeper than for the pelleted catalyst. At low bed height the effect of this steep portion was more pronounced, due to the increasing difference in temperature between the bulk of the bed and wall. This feature probably corresponds to non-uniformity in the velocity profiles due to the packing. Schertz and Bischoff (1969), Dorweiler and Smith (1959), Ahmed and Fahien (1980) and Morales et al. (1951) measured radial velocity profiles down stream from the packing by means of long circular hot wire loop, located at fixed radii. They all reported that the velocity profiles increased at the wall and then decreased monotonically.

The profiles obtained at elevated pressures tend to be flatter at the center of the reactor and give a steeper drop near the wall than the profiles at atmospheric pressure. It can also be observed, that the radial temperature profiles in the center of the reactor using a monolith catalyst at elevated pressure are flatter and smoother than those pelleted catalysts especially at 20 bars.

The magnitude of the temperature differences at elevated pressures at distance 2.5 to 5.0 mm from the wall were of the order of 30 ^{o}C to 70 ^{o}C for monoliths and 10 ^{o}C to 40 ^{o}C for

pelleted catalyst, (*i.e.*, up to 77% of the total temperature difference for monolith catalysts and 50% for the pelleted catalyst). These suggest that the major resistance to radial heat transfer is at the wall. At atmospheric pressure, however, the corresponding temperature differences were about 8 °C to 22 °C for the catalyst pellets and were unpronounced in the case of the monolith catalyst. The differences between the temperatures at the center of the bed for shallow beds (0.15m), and the deepest beds (0.30m) at 1, 11 and 20 bars are 22 °C, 31 °C and 39 °C for monoliths and 34 °C, 37 °C and 40 °C for the (3.175*3.175) mm pellets catalyst bed respectively.

Experimental results for wall heat transfer coefficients were obtained using pellets and monoliths catalysts in the fixed bed with air as the fluid medium at atmospheric and high pressure are shown in Figures 10 and 11. The results presented in Figure 10 show the wall heat transfer coefficient plotted against particle Reynolds number for pelleted catalyst.

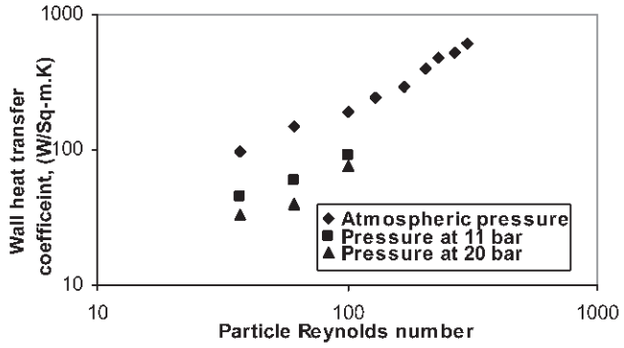

Figure 10. Effect of pressures on wall heat transfer coefficient for (3.175*3.175) mm using air

Figure 11 shows the variation of wall Nusselt number with channel Reynolds number ($Re_c = GD_h/\mu$) of the monolithic structure.

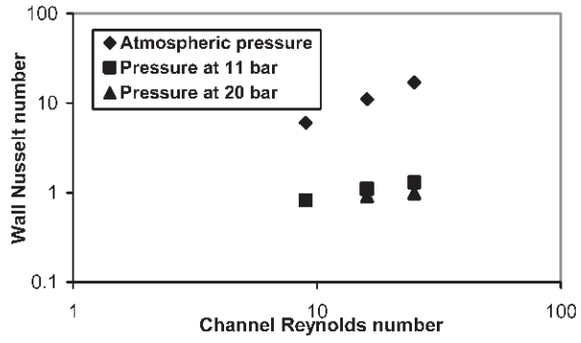

Figure 11. Effect of atmospheric and higher pressures on wall Nusselt number for monolith

From these Figures, it is obvious that the general trend of the plots are almost the same in that the wall heat transfer coefficient increases with increasing practical or channel Reynolds number. Moreover, in these Figures, the atmospheric pressures values lie well above those obtained at higher pressures, indicating that pressures higher than atmospheric decrease the

wall heat transfer. This influence could be due to the increased thickness of the boundary layer at the wall tube, which may prevent the heat transfer from the wall.

Figures 12 and 13 show values of the wall Nusselt number ($Nu=h_w D_p/k_f$) plotted as a function of particle Reynolds for air, carbon dioxide and helium at atmospheric pressure and air at high pressures. In Figure 12 there are significant differences between the values for the three gases. Therefore, the reasonable predictions it is necessary to obtain separate correlations for each gas. For the higher pressures of 11 and 20.7 bars, one correlation was established for both pressures and pellets by using regression methods with an accuracy of 94%.

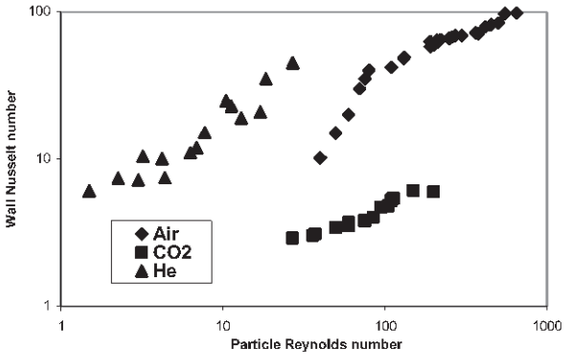

Figure 12. Correlation of wall Nusselt number for three different gasses

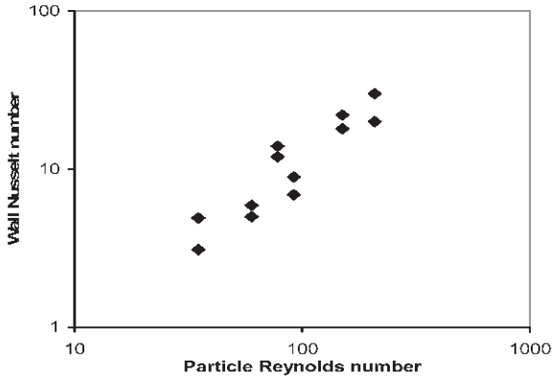

Figure 13. Correlation of wall Nusselt number for high pressure

Using regression analysis the correlations at atmospheric pressure for the three gases and for air at high pressures are presented in the following table:

Table 1. Correlations obtained at atmospheric and high pressure

Fluid	Pressure	Correlations
Air	Atmospheric	$Nu = 2.09\ (Re_p)^{0.438}\ (D_r/D_p)^{-0.301}$
Co_2	Atmospheric	$Nu = 1.65\ (Re_p)^{0.5}\ (D_r/D_p)^{-0.44}$
He	Atmospheric	$Nu = 42.52\ (Re_p)^{0.48}\ (D_r/D_p)^{-0.784}$
Air	High	$Nu = 4.17\ (Re_p)^{0.432}\ (D_r/D_p)^{-0.854}$

Figure 14 compares some experimental correlations of wall Nusselt number with the present correlation obtained for air at atmospheric pressure. As might be expected from the different conditions of the experimental studies, wide variations between correlations can be observed in this plot. These differences may be due to the spherical and cylindrical packing as well as the fluid medium which gave different results for the wall heat transfer coefficient results for the wall heat transfer coefficient. Hanratty (1954) and, Li & Finlayson (1977) have pointed out that there is some evidence that heat transfer from the wall is different with spherical and cylindrical particles. Note that in the case of spherical packing only point contacts with the wall are involved, so that less obstructed flow near the wall in a bed of spheres made the transport to the wall more like that in an empty tube. In the case of cylinders, on the other hand, planer contact is more likely and the heat transfer coefficients could be larger.

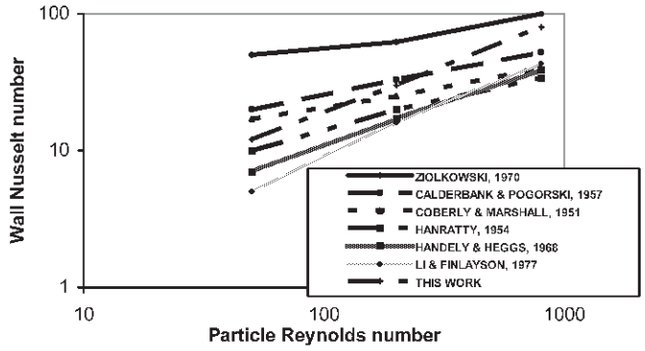

Figure 14. Some reported correlations for wall Nusselt number with present correlation

Figure 15 shows the variation in a wall heat transfer coefficient with channel number of the monolithic structure, in which the heat transfer is seen to increase slightly with increasing channel Reynolds number. This may be due to the increase in the level of laminar flow through the passages tending to reduce the thickness of the boundary layer at wall of the channels thus improving the rate of heat transfer through the bed and increasing the value of the wall heat transfer coefficient. As might be expected, the heat capacity and thermal conductivity of the fluid has an effect on the wall heat transfer coefficient. This Figure indicates also that the extrapolated values of helium are higher than the values of air and carbon dioxide.

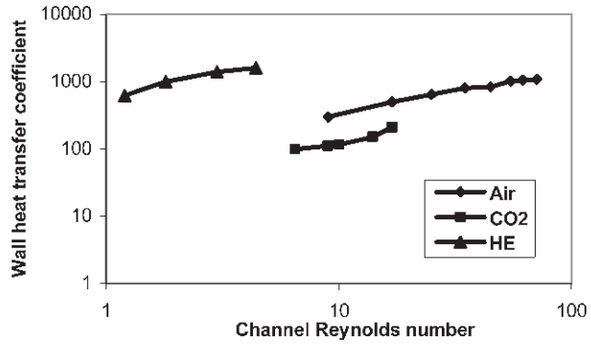

Figure 15. Variation of wall heat transfer with channel Reynolds number for of gases

Figure 16 shows plots of the wall Nusselt number for monolith against channel Reynolds number of the present work and other workers. The correlation of Votruba et. al. (1975) for a metal monolith suggests that the wall Nusselt number increases with increasing channel Reynolds number, while Hawthorn's data show no increase with increasing Reynolds number. Considerable differences in the wall Nusselt number are apparent between the correlations and the present work. However, the trend of the correlation of Votruba et. al. (1975) is almost the same as the present study for the three different gases. Votruba's correlation is in fair agreement with the results for the Nusselt number obtained for carbon dioxide in the present paper. The differences between the results for air and helium and Votruba's correlations may be due to the structure of the matrices since the void fraction used by Votruba et. al. was in the range of 0.6 to 0.61 and for Hawthorn is 0.61, while for the present work is 0.78. Also the shape of the channels important for heat transfer through the walls.

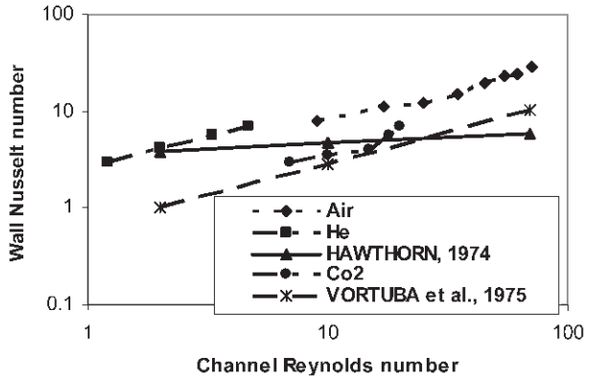

Figure 16. Correlation of present wall Nusselt number with published correlations for monoliths

Figure 17 shows the comparison of wall Nusselt numbers of the bed monoliths with a packed bed of nickel alumina pellets (3.175*3.175) mm with air, carbon dioxide and helium flowing through the beds at atmospheric pressure. In these three gases, the pellet Nusselt number shows higher values than the monolith Nusselt at a given mass flow rates. These expected differences may be due to the effects of the bed monolith geometry in which the large voidage will provide less resistance. Also the hydraulic radius of monolith catalyst was much smaller than pellet diameter.

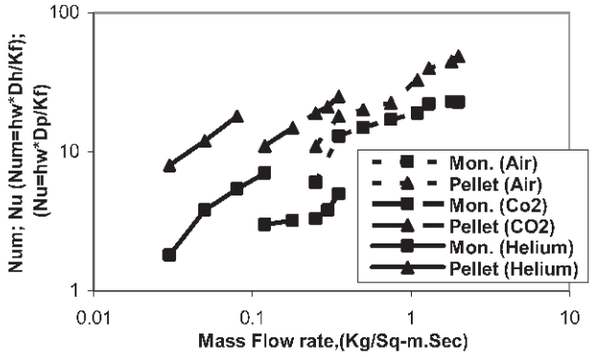

Figure 17. Comparison of wall Nusselt number of monolith with Nusselt number of pellet

ACKNOWLEDGMENTS

The authors gratefully acknowledge the financial support of the present work by the Al-Mergheb University

NOMENCLATURE

a_n	n^{th} root of Bessel function of first order and first kind	(--)
A_1	Wall tube surface area	(m^2)
A_2	Thickness area	(m^2)
A_3	Inside tube surface area	(m^2)
C_p	Specific heat of the gas.	(J/kg.K)
D_h	Hydraulic diameter of monolith structure hole.	(m)
D_p	Particle diameter.	(m)
D_t	Tube diameter.	(m)
G	Fluid mass flux.	(kg/m^2.sec)
h_w	Wall heat transfer coefficient.	(W/m^2.K)
J_o	Bessel function of zero order and first kind.	(--)
J_1	Bessel function of first order and first kind	(--)
K_{er}	Effective radial thermal conductivity.	(W/m.K)
K_{ea}	Effective axial thermal conductivity.	(W/m.K)
M	Number of total exit temperature.	(---)
N	Number of the depth	(--)
Nu	Nusselt number for pellet= (h_w*D_p/K_f)	(--)
Nu_m	Nusselt number for monolith catalyst= (h_w*D_h/K_f)	(--)
R_t	Tube radius.	(m)
r	Radial coordinates.	(m)
T	Temperature.	(^oC)
T_w	Wall temperature tube.	(^oC)
T_o	Bed inlet temperature.	(^oC)
$T_{Theo.}$	Theoretical temperature.	(^oC)
T_{exp}	Experimental temperature.	(^oC)
Z	Axial coordinate (bed depth).	(m)
β	Biot number = (h_w*R_t/K_{er})	(--)
R_{ep}	Particle Reynolds number = ($G*D_p/\mu_g$)	(--)
R_{eC}	Channel Reynolds number=($G*D_h/\mu_g$)	(--)
μ_g	Dynamic viscosity of the gas.	(Pa.Sec)

REFERENCES

1. Ahmed, M. & Fahien, R. W., (1980) "Tubular Reactor Design I – Two Dimensional Model", *Chem. Eng. Sci.*, 35, 889-895.
2. Al-Meshragi, M. & Hughes, R., (2001) "An Experimental Investigation of the Radial Heat Transfer in Fixed Beds at Atmospheric and High Pressure", *51st Canadian Chemical Engineering Conference, Halifax, Canada, October 14-17*, No. (384).
3. Balakotaiah, V. & Dommeti, S. M. S., (1999) "Effective Models for Packed Bed Catalytic Reactors", *Chem. Eng. Sci.*, 54, 162-168.
4. Benneker, A.H., Kronberg, A.E., Lansbergen, I. C. & Westerterp, K. R., (2002) "Mass Dispersion in Liquid Flow Through Packed Beds", *Ind. Eng. Res.*, 41, 1716.
5. Coberly, C. A. & Marshall, W. R. (1951), "Temperature Gradient in Gas Stream Flowing Through Fixed Granular Beds", *Chem. Eng. Prog.*, **47**, 141-150.
6. Dixon, A.G. & Cresswell, D.L., "Theoretical Prediction of Effective Heat Transfer Parameters in Packed Beds", *AIChE J*, 25, 663-676 (1979).
7. Dixon, A. G. (1988), "Correlation for Wall and Particle Shape Effects on Fixed Bed Bulk Voidage", *Canadian Journal of Chemical Eng.*, 66, 705-708.

8. Dorweiler,V.P. & Smith, J.M., (1959) "Mass Transfer at Low Flow Rates in a Packed Column", *AIChE J*, 5, 139-144.
9. Hanratty, T.J., (1954) "Nature of Wall Heat Transfer Coefficient in Packed Beds", *Chem. Eng. Sci*., 3, 209-214.
10. Kronberg, A. E. & Westerterp, K. R., (1999) "Non-Equilibrium Effects in Fixed-Bed Interstitial Fluid Dispersion", *Chem. Eng. Sci*., 54, 3977-3993.
11. Li, H. & Finlayson, B.A., (1977) "Heat Transfer in Packed Beds- a Reevaluation", *Chem. Eng. Sci*., 32, 1055-1066.
12. Morales, M., Spinn, C.W. & Smith, J. M., (1951) "Velocities and Effective Thermal Conductivities in Packed Beds", *Industrial and Engineering Chemistry*, 43, 225-232.
13. Votruba, J., Mikus, O., Halavalek, V. & Skrivanek, J., (1975) "Heat and Mass Transfer in Honeycomb Catalysts-II", *Chem. Eng. Sci*., 30, 201-206.
14. Schertz, W. W. & Bischoff, K. B., (1969) "Thermal and Material Transport in Nonisothermal Packed Beds", *AIChE J*., 15, 597-604.

Al-Meshragi, M. & Hughes, R., Journal of the Association of Arab Universities for Basic and Applied Sciences, Vol.3, 2007, 32-47

دراسة الانتقال الحراري الجداري في مفاعل قاعي عند مستوى الضغط والضغط المرتفع

[*]المشرقي، م و [**]هوجز، ر
قسم الهندسة الكيميائية، كلية الهندسة، جامعة المرقب، الخمس، ليبيا
قسم الهندسة الكيميائية، جامعة سالفورد، مانشستر، بريطانيا

الملخص

في هذا البحث تم قياس معامل الانتقال الحراري عند جدار قاع ثابت باستخدام الهواء وثاني أكسيد الكربون وغاز الهيليوم لمحفزات معينة. كما تم دراسة المعامل الحراري عند ضغط يصل إلى 20 بار في هذا النظام. كما تم تحليل نتائج التدرج الحراري من خلال التجارب باستخدام نموذج متجانس لأجل تحديد قيم معامل الانتقال الحراري بين الجدران. وخلص البحث إلى أن معامل الانتقال الحراري يزداد بازدياد رقم رينولد في كل من الضغطين (الجوي والمرتفع)، وإن تأثير الضغط على الانتقال الحراري بين الجدران، كدالة في رقم رينولد، يعطي الانطباع أن الضغوط التي تزيد على الضغط الجوي تسبب نقصاناً في الانتقال الحراري، كما أن قيم الضغط الجوي تتفوق كثيراً على تلك الخاصة بالضغوط المرتفعة.